1   **Title:** Susceptible host availability modulates climate effects on dengue dynamics

2   **Authors:** Nicole Nova[1*], Ethan R. Deyle[2,3], Marta S. Shocket[1,4],

3   Andrew J. MacDonald[1,5], Marissa L. Childs[6], Martin Rypdal[7],

4   George Sugihara[2], and Erin A. Mordecai[1]

5   **Affiliations:**   [1]Department of Biology, Stanford University, Stanford, CA, USA.

6   [2]Scripps Institution of Oceanography, University of California San

7   Diego, La Jolla, CA, USA.

8   [3]Department of Biology, Boston University, Boston, MA, USA.

9   [4]Department of Ecology and Evolutionary Biology, University of

10   California, Los Angeles, CA, USA.

11   [5]Earth Research Institute & Bren School of Environmental Science and

12   Management, University of California Santa Barbara, Santa Barbara,

13   CA, USA.

14   [6]Emmett Interdisciplinary Program in Environment and Resources,

15   Stanford University, Stanford, CA, USA.

16   [7]Department of Mathematics and Statistics, UiT The Arctic University

17   of Norway, Tromsø, Norway.

18   ***Correspondence:** Nicole Nova, Department of Biology, Stanford University

19   Address: 327 Campus Drive, Stanford, CA 94305-5020

20   **Email:** nicole.nova@stanford.edu

21   **Emails of co-authors:** In order of co-authorship after first author,

22   ethan.deyle@gmail.com, marta.shocket@gmail.com, andy.j.macdon@gmail.com,

23 marissac@stanford.edu, martin.rypdal@uit.no, gsugihara@ucsd.edu,

24 emordeca@stanford.edu

25 **Keywords:** Arbovirus, climate, dengue, empirical dynamic modeling, forecasting,

26 mosquito-borne disease, rainfall, susceptible population size, temperature

27 **Short running title:** Ecological drivers of dengue

28 **Type of article:** Letter

29 **Statement of authorship:** NN, ERD, EAM, GS, and MR conceived the idea for the

30 study and designed the analyses. MR inferred the proxy for susceptible population

31 size time series. NN, ERD, MSS, AJM, and MLC performed the analyses. NN wrote the

32 first draft of the manuscript. All authors contributed to manuscript revisions and

33 gave approval for publication.

34 **Data accessibility statement:** The data used in this study is publicly available

35 (http://dengueforecasting.noaa.gov/). A combined version of the dataset used in

36 this study was obtained from Johnson *et al.* (2018)

37 (https://github.com/lrjohnson0/vbdcast). Code and formatted data used in this

38 study is available on Github: https://github.com/nicolenova/EDMdengue

39 **Number of words in the abstract:** 147

40 **Number of words in the main text:** 5,148

41 **Number of references:** 66

42 **Number of figures/tables/boxes:** 6

Abstract

Experiments and models suggest that climate affects mosquito-borne disease transmission. However, disease transmission involves complex nonlinear interactions between climate and population dynamics, which makes detecting climate drivers at the population level challenging. By analyzing incidence data, estimated susceptible population size, and climate data with methods based on nonlinear time series analysis (collectively referred to as empirical dynamic modeling), we identified drivers and their interactive effects on dengue dynamics in San Juan, Puerto Rico. Climatic forcing arose only when susceptible availability was high: temperature and rainfall had net positive and negative effects, respectively. By capturing mechanistic, nonlinear, and context-dependent effects of population susceptibility, temperature, and rainfall on dengue transmission empirically, our model improves forecast skill over recent, state-of-the-art models for dengue incidence. Together, these results provide empirical evidence that the interdependence of host population susceptibility and climate drive dengue dynamics in a nonlinear and complex, yet predictable way.

INTRODUCTION

In concert with globalization and climate change, mosquito-borne diseases, and dengue in particular, are (re)emerging globally and spreading to higher latitudes (Kilpatrick & Randolph 2012; Ryan *et al.* 2019). Dengue virus—vectored primarily by urban *Aedes aegypti* (Kraemer *et al.* 2015)—places half of the global human population in 128 countries at risk of infection (Brady *et al.* 2012; Kraemer *et al.* 2019). In the absence of effective vaccines or treatments (Katzelnick *et al.* 2017a; Sridhar *et al.* 2018), public health agencies rely on vector control to reduce dengue transmission (Erlanger *et al.* 2008). Effective vector control interventions require understanding the mechanisms linking climate, vector ecology, disease transmission, and host population susceptibility to better predict disease outbreaks—a major challenge.

Since *Aedes* spp. mosquitoes are sensitive to climate, including temperature and rainfall (Stewart Ibarra *et al.* 2013; Mordecai *et al.* 2019), we expect temperature and rainfall to be important drivers of dengue outbreaks. Although temperature affects mosquito and viral traits in laboratory experiments (Watts *et al.* 1987; Lambrechts *et al.* 2011; Mordecai *et al.* 2017), the relationship between temperature and dengue incidence in the field has been ambiguous (Caldwell *et al.* 2020). Thus, temperature-dependent models have had mixed success predicting the timing and magnitudes of epidemics (Hii *et al.* 2012; Johansson *et al.* 2016; Johnson *et al.* 2018). The rainfall–dengue relationship is also complex. Rainfall can fill container-breeding habitats for mosquitoes, increasing mosquito abundance and

81 dengue incidence (Stewart Ibarra *et al.* 2013). Low rainfall can also facilitate dengue

82 transmission by promoting water storage that serves as standing-water habitat for

83 mosquitoes (Oliveira-lima *et al.* 2000), and heavy rainfall can reduce mosquito

84 abundance by flushing out larvae (Koenraadt & Harrington 2008). The net effect of

85 climate on dengue depends on many different mechanisms and is highly context-

86 dependent.

87   Disease incidence also depends nonlinearly on susceptible availability,

88 because epidemic growth slows as the population of susceptible individuals is

89 exhausted (Anderson & May 1979; Dushoff *et al.* 2004; Mina *et al.* 2015; Pitzer *et al.*

90 2015; Rypdal & Sugihara 2019). Further, susceptible availability may influence the

91 effects of climate on dengue dynamics. However, such interactive effects are difficult

92 to detect since susceptibility is difficult to observe, especially in endemic settings

93 where multiple serotypes circulate and create a complex landscape of time-

94 dependent and serotype-dependent immunity (Katzelnick *et al.* 2017b). Specifically,

95 four serotypes of dengue regularly circulate in many regions: each provides long-

96 term serotype-specific (homologous) immunity and short-term (heterologous)

97 cross-protection against other serotypes (dos Santos *et al.* 2017; Jiménez-Silva *et al.*

98 2018; Hamel *et al.* 2019). Following a brief period of cross-protection, antibodies at

99 a mid-range of titers can cause antibody-dependent enhancement of disease

100 following heterologous, secondary infection, until titers decay to the point of nearly

101 full heterologous susceptibility (Katzelnick *et al.* 2017b). Given this complex and

102 dynamic immune landscape, directly detecting population susceptibility to

103 circulating dengue virus at any point in time is difficult without longitudinal

104 serology studies, which are not widely available (Gordon *et al.* 2013; Katzelnick *et*

105 *al.* 2017b).

106   Previous prediction models of dengue outbreaks used phenomenological

107 (Johansson *et al.* 2009b; Hii *et al.* 2012; Johnson *et al.* 2018) and mechanistic

108 equation-based approaches (Tran *et al.* 2013; Liu-Helmersson *et al.* 2014; Morin *et*

109 *al.* 2015; Mordecai *et al.* 2017), which may not fully capture interdependence

110 between climate and susceptible availability. Phenomenological models may

111 underperform when extrapolating past observed contexts, and equation-based

112 mechanistic models rely on parameter estimates from laboratory studies

113 engineered to isolate single mechanisms producing separate relationships between

114 drivers and outcome, eliminating the complex interdependence at the population

115 level. While laboratory studies provide robust validation of mechanisms

116 (Lambrechts *et al.* 2011), the fixed relationships obtained from them do not

117 necessarily translate into robust causal understanding for the complexity of field

118 systems (Sugihara *et al.* 2012). Even if causality exists between two variables in such

119 a system, their correlation can switch signs during different time periods, resulting

120 in a net correlation of zero (Deyle *et al.* 2016b). This temporal variation in the

121 direction of correlation results from the nonlinear, state-dependent relationship

122 between the variables. Conversely, even if two variables are consistently correlated,

123 the association could be spurious due to a confounder.

124   To overcome these challenges, we used empirical dynamic modeling (EDM)

125 (Sugihara *et al.* 2012)—a mechanistic, equation-free, data-driven approach that

126   accounts for the context-dependence of ecological drivers to identify and model

127   mechanisms driving dengue epidemics. EDM is based on reconstructing system

128   dynamics evident in time series, without assuming fixed relationships. Relationships

129   among variables can change through time if interactions among variables are

130   context-dependent. EDM does not require assumptions about the functional form of

131   the model, but instead derives dynamic relationships empirically by constructing an

132   attractor—a geometric object (i.e., curve or manifold) that embodies the rules for

133   how relationships among variables change with respect to each other through time

134   depending on system state (location on the attractor)—from time-series

135   observations. Like a set of equations, the attractor encompasses the dynamics of a

136   system, and thus can provide a mechanistic understanding of the system that is

137   derived empirically, without requiring an *a priori* assumed set of equations.

138   Here, we used EDM and a proxy for susceptible population size (Rypdal &

139   Sugihara 2019) to answer three questions: (1) Do temperature, rainfall, and/or

140   inferred susceptible availability drive population-level dengue incidence? (2) Can

141   we predict dengue dynamics using temperature and rainfall data and inferred

142   susceptible availability? (3) What is the functional form of each climate–dengue

143   relationship at the population level, and how is this relationship influenced by

144   susceptible availability?

METHODS

Time series data

We obtained time series of weekly observations of dengue incidence (total number

of new cases of all serotypes), average temperature (℃), and total rainfall (mm) in

San Juan, Puerto Rico, for 19 seasons (1990/1991–2008/2009) spanning calendar

week 18, 1990 to week 17, 2009 (Figure 1a–c) from the National Oceanic and

Atmospheric Administration in November 2016

(http://dengueforecasting.noaa.gov/). We obtained data for four additional seasons

(2009/2010–2012/2013) from Johnson *et al.* (2018) in April 2020

(https://github.com/lrjohnson0/vbdcast). Although dengue incidence data were

also available for Iquitos, Peru (Johansson *et al.* 2019), we chose to focus on San

Juan because the time series was longer, and therefore more amenable to EDM

analyses (Munch *et al.* 2020).

Direct measurements of susceptible availability are not available, so from

weekly incidence data $I(t)$, we estimated time-dependent growth rates: $\lambda = I(t + \Delta t)/ I(t)$. The growth rate, λ, is proportional to the effective reproduction

number, R_{eff}, and equivalent to R_{eff} if Δt equals the average time between primary

and secondary host infections. Vector-borne disease models show that R_{eff} is

proportional to the geometric mean of the susceptible host population and the

susceptible vector population: $R_{\text{eff}} = \sqrt{S_{\text{h}}S_{\text{v}}}\, R_0$, where R_0 is the basic reproduction

number (Zhao *et al.* 2020). Hence, $\lambda \propto \sqrt{S_{\text{h}}S_{\text{v}}}$ and λ can be used as a proxy for the

166   susceptible population size at least during inter-outbreak periods where the

167   transmission rate and R_0 can be assumed to vary very little (Rypdal & Sugihara

168   2019).

169   We estimated λ by linear regression using the model $I(t + \Delta t) = \lambda\, I(t)$ for

170   12 time points in a 12-week running window ($\Delta t = 1$ week). The model is robust to

171   the window size (Rypdal & Sugihara 2019). In the discrete case, when $\lambda < 1$ the

172   system is stable (inter-outbreak period) and when $\lambda \geq 1$ then the system is unstable

173   (outbreak period) (Supporting Information). We treated the resulting time series of

174   λ, hereafter "susceptibles index" (Figure 1d), as a proxy for the susceptible

175   population size when $\lambda < 1$, and a proxy for the combined effects of susceptible

176   availability and R_0 when $\lambda \geq 1$.

Empirical dynamic modeling (EDM)

178   EDM infers a system's mechanistic underpinnings and predicts its dynamics using

179   time series data of one or more variables to construct an attractor in state space

180   (Figure S1). This procedure is called univariate (using lagged versions of a single

181   variable time series) or multivariate state-space reconstruction (SSR). Properties of

182   the attractor are assessed to examine characteristics of the system (Deyle &

183   Sugihara 2011). We normalized each time series to zero mean and unit variance to

184   remove measurement unit bias, ensuring the variables would be comparable and

185   the attractor would not be distorted. All analyses were conducted in R version 3.5.1

186   (R Development Core Team 2018) and all EDM analyses were performed using

187   package `rEDM` (Park *et al.* 2020).

188   To infer mechanisms, EDM should be applied in systems where there is

189   evidence of underlying low-dimensional deterministic dynamics (Cummins *et al.*

190   2015). EDM assumptions are met when stochasticity is present (e.g., due to

191   measurement noise, stochastic drivers, or unexplained variability) (Cenci *et al.*

192   2019; Munch *et al.* 2020), but the system cannot be entirely stochastic. To test for

193   low-dimensional deterministic dynamics we performed univariate SSR for each

194   variable, and used *simplex projection* (Sugihara & May 1990)—a type of nearest

195   neighbor regression performed on an attractor—to check whether the system is

196   forecastable beyond the skill of an autoregressive model—an indicator of

197   underlying deterministic dynamics (Figures S2a and S4; Supporting Information).

198   To test for nonlinear state dependence of a variable—the motivation behind EDM—

199   we used the *S-map* test for nonlinearity (Sugihara 1994) (Figures S2b, c and S5;

200   Supporting Information).

201   **EDM—Convergent cross-mapping**

202   We used an EDM approach called *convergent cross-mapping* (CCM) (Sugihara *et al.*

203   2012) to identify drivers of dengue incidence. If two variables are causally related,

204   then a multivariate attractor—where each variable in the system represents a

205   dimension that traces the dynamics of the system—can be reconstructed (up to a

206   practical limit) using lagged versions of just one of the variables (Figure S1). Based

10

207   on Takens' Theorem, this univariate "shadow attractor" preserves the structural and

208   dynamic properties of the original multivariate attractor (Takens 1981; Sugihara *et*

209   *al.* 2012). The concept behind CCM is that if temperature causes dengue incidence,

210   then information about past temperature will be embedded in the dynamics of

211   dengue, such that the shadow attractor produced using only incidence data allows

212   us to accurately reconstruct temperature in the past. However, the converse

213   scenario would not be true: since dengue does not cause temperature, the shadow

214   attractor constructed using temperature data should not contain information to

215   accurately reconstruct past dengue incidence (Supporting Information).

216   The critical criterion for estimating causal (directional) associations between

217   two variables using CCM is checking that the cross-mapping skill (i.e., Pearson's

218   correlation coefficient, ρ, between predicted driver values using the univariate SSR

219   of the response variable, and the observed driver values) monotonically increases

220   and plateaus (i.e., converges) with the length of the response variable time series

221   used in cross-mapping. We used the Kendall's τ test as a significance test for

222   convergence of cross-mapping skill using the `Kendall` package (McLeod 2011). If

223   $\tau > 0$ then there is convergence (Grziwotz *et al.* 2018).

224   We performed pairwise cross-correlations on the time series to investigate

225   time-lagged relationships between potential drivers (i.e., temperature, rainfall, and

226   susceptibles index) and dengue incidence using the `tseries` package (Trapletti &

227   Hornik 2018). Based on these analyses (Figure S6), we applied a 9-week time lag

228   between temperature and incidence, an averaged lag of 3–9 weeks for rainfall (i.e.,

11

229   the average rainfall over the preceding 3–9 weeks) to resemble standing water as

230   mosquito breeding habitat over a longer time period, and a 5-week lag for the

231   susceptibles index. These lags are proxies for the time delays of potential cause-and-

232   effects and are consistent with results from field studies (Chen *et al.* 2010; Stewart

233   Ibarra *et al.* 2013).

234   We assessed the strength of evidence for effects of potential drivers on

235   dengue by comparing the CCM performance using the data with the performance of

236   two null models that control for the seasonal trend (i.e., interannual mean) observed

237   in all variables (Figure 2). These null models address the sensitivity of CCM to

238   periodic fluctuations (i.e., seasonality), which can make two variables appear to be

239   causally linked when instead they are simply synchronized by a seasonal

240   confounder (Cobey & Baskerville 2016; Deyle *et al.* 2016a). In the first "seasonal"

241   null model, we preserved the seasonal signal, but randomized the interannual

242   anomalies (Deyle *et al.* 2016a). In the second, more conservative "Ebisuzaki" null

243   model, we conserved any periodicity (beyond seasonal) and randomized the phases

244   of Fourier-transformed time series (Ebisuzaki 1997). We tested for statistically

245   significant differences in cross-mapping skill between the model that used the data

246   *versus* the null models by performing Kolmogorov-Smirnov (K-S) tests after

247   convergence.

248   We also repeated CCM in the nonsensical, reverse-causal direction (e.g., to

249   test whether incidence drives climate) as a control for potential spurious

250   relationships generated by non-causal covariation (e.g., due to seasonality). This

251 addresses the issue of synchrony, in which CCM can indicate bidirectional causality

252 when one direction is false or nonsensical (Baskerville & Cobey 2017; Sugihara *et al.*

253 2017).

254 **EDM—Forecast improvement**

255 We examined the predictive power of the drivers on dengue incidence by assessing

256 how well we can predict dengue dynamics using temperature, rainfall, susceptibles

257 index, and their combined effects. We used a combination of univariate SSR (i.e.,

258 with incidence data) and multivariate SSR to build forecasting models and to

259 determine the improvement of forecasting using simplex projection when including

260 different combinations of drivers (Dixon *et al.* 1999; Deyle *et al.* 2013, 2016a)

261 (Supporting Information). We built the SSR forecasting models/attractors using the

262 1990/1991–2008/2009 season data (Figure 1) and made forecasts 8 weeks ahead.

263 We assessed model forecasting performance using leave-one-out cross-validation.

264   Next, we evaluated out-of-sample forecasting performance of these models

265 using testing data from four additional seasons (2009/2010–2012/2013).

266 Predictions made on week zero for the first forecast of the 2009/2010–2012/2013

267 period (8 weeks ahead) came only from SSR using the 1990/1991–2008/2009 data.

268 All subsequent weekly forecasts (8 weeks ahead) were made from updated SSR

269 using all previous data, including past observations from the testing dataset.

270   Forecast uncertainty was evaluated by taking the density and morphology of

271   the attractor into account. The more compact a simplex was and the less its starting

272   position on the attractor mattered for the simplex projection, the more certain we

273   were about our point estimate. Forecast variance was obtained from a distribution

274   of weighted nearest neighbor regression from edges of simplexes constructed at

275   various starting positions in the past.

276   Finally, we compared our top model performance with performance of

277   previous models from 16 teams that participated in a dengue forecasting challenge

278   (Johansson *et al.* 2019) and had access to the same data. To make a fair comparison,

279   we followed the procedure as directed in the challenge (Supporting Information).

280   **EDM—Scenario exploration**

281   In nonlinear systems, drivers generally have an effect that is state-dependent: the

282   strength and direction of the effect depends on the current state of the system.

283   Scenario exploration with multivariate EDM allowed us to assess the effect of a

284   small change in temperature or rainfall on dengue incidence, across different states

285   of the system. The outcome of these small changes allowed us to deduce the

286   relationship between each climate driver and dengue incidence and how they

287   depend on the system state. For each time step t we used S-maps (Sugihara 1994;

288   Deyle *et al.* 2016a) to predict dengue incidence using a small increase ($+\Delta X$) and a

289   small decrease ($-\Delta X$) of the observed value of driver $X(t)$ (temperature or rainfall).

290   For each putative climate driver, the difference in dengue predictions between these

14

291   small changes is $\Delta Y = Y(t+1)\left[X(t) + \frac{\Delta X(t)}{2}\right] - Y(t+1)\left[X(t) - \frac{\Delta X(t)}{2}\right]$, where $Y(t +$

292   1) is a function of X and all other state variables, and we used $\Delta Y / \Delta X$ to approximate

293   the effect of driver X at time t. We repeated this over all time steps in our time series

294   for both temperature and rainfall to recover their approximate relationships with

295   dengue incidence at different states of the system. Scenario exploration analyses

296   were repeated across several model parameterizations to address potential

297   sensitivity to parameter settings (Supporting Information).

298   **RESULTS**

299   **Drivers of dengue dynamics**

300   EDM showed that temperature, rainfall, and the susceptibles index drive dengue

301   incidence since the convergence criterion was met (Kendall's $\tau > 0$, $P < 0.01$) in all

302   three cases (Figure 3a–c). Rainfall and susceptibles index were significant drivers of

303   dengue incidence beyond seasonality, as their effects were distinguishable from

304   seasonal and Ebisuzaki null models (Figures 3b–c and S8b–c; K-S $P < 0.0001$). This

305   implies statistically significant effects of both rainfall and the susceptibles index on

306   dengue, which are not obscured by a periodic confounder. However, temperature

307   was not a significant driver beyond seasonality (Figures 3a and S8a; K-S $P = 0.90$).

308   We cannot rule out the possibility that the apparent forcing of temperature on

309   dengue is due to a seasonal confounder. However, if no such confounder exists, then

310   the seasonal trend in temperature, which accounts for most temperature variation

311   in San Juan, drives the seasonal trend observed in dengue incidence. Compared to

312   the other drivers, the converging cross-mapping skill of the temperature null

313   models were relatively high (Figures 3 and S8), suggesting that temperature

314   seasonality in each null model was a strong driver. Thus, seasonal temperature may

315   be driving dengue dynamics, a result consistent with other studies (Huber *et al.*

316   2018; Robert *et al.* 2019).

317   As expected, EDM tests for putative causality in the nonsensical directions—

318   incidence driving temperature or rainfall—were not significant (i.e., no

319   convergence; Figure S7, black lines). This result further supports the finding that

320   temperature and rainfall drive dengue incidence, because their causal relationships

321   were not confounded by spurious bidirectionality. The null models for the

322   nonsensical directions of causality (Figure S7, grey lines) also displayed no

323   convergence (completely flat), as expected (i.e., seasonality of dengue incidence

324   does not drive seasonality of temperature or rainfall). However, seasonality (or any

325   periodicity) of temperature, rainfall and susceptibles index drive dengue dynamics,

326   shown by convergence of the seasonal and Ebisuzaki null models (grey lines in

327   Figures 3 and S8).

328   **Predictive power of drivers**

329   The multivariate SSR model using only temperature and rainfall data did not predict

330   dengue incidence very well (ρ = 0.3839, RMSE = 47.72) although it captured the

331   seasonality of the epidemics (Figure 4a). Forecasting skill doubled when the

332   susceptibles index was included along with rainfall and temperature (ρ = 0.7547,

333   RMSE = 37.40; Figure 4c), where timing and magnitude of epidemics were captured

334   reasonably well. Dengue incidence prediction improved even further when

335   incidence was added into the model with all drivers (ρ = 0.7662, RMSE = 37.14;

336   Figure 4e). Dengue incidence was somewhat predictable using univariate SSR of

337   incidence data alone (ρ = 0.4459, RMSE = 46.75; Figure 4g), suggesting that the

338   dengue incidence time series contains information about its drivers, although

339   limited. This points to some additional value of including the driver variables.

340   We also evaluated the performance of the SSR models (Figure 4a, c, e, g)

341   constructed using data from seasons 1990/1991–2008/2009 on external, testing

342   data from 2009/2010–2012/2013 that were not used in SSR (Figure 4b, d, f, h). The

343   average out-of-sample forecasting skill for each model for the testing seasons was

344   higher than that of the 1990/1991–2008/2009 forecasts, although the errors were

345   larger. The model using only temperature and rainfall displayed predictability (ρ =

346   0.8989, RMSE = 52.30; Figure 4b), the model that also included the susceptibles

347   index improved predictions (ρ = 0.9475, RMSE = 52.12; Figure 4d), and the model

348   that also included past incidence made highly accurate predictions (ρ = 0.9697,

349   RMSE = 46.75; Figure 4f). The model that only included dengue incidence without

350   the drivers was also predictive, although more error-prone (ρ = 0.9044, RMSE =

351   57.34; Figure 4h). All SSR models (Figure 4a–h) had significant forecasting skill (ρ)

352   values (Fisher's z-transformation P < 0.001).

353   The model with the highest prediction skill for the testing seasons

354   (2009/2010–2012/2013), which included past climate, susceptibles index, and

355   incidence data as predictors (Figure 4f), also outperformed models from the dengue

356   forecasting challenge, including the ensemble model (Johansson *et al.* 2019) for

357   predicting peak incidence, peak week, and seasonal incidence for all seasons on

358   average (Tables S1–S2, Figures S9–S12). This demonstrates the benefit of the EDM

359   approach for capturing the mechanistic, nonlinear, interdependent relationships

360   among drivers over both equation-based mechanistic models and phenomenological

361   models.

362   **State-dependent functional responses**

363   As expected, we find state-dependent effects of temperature and rainfall with non-

364   zero median effects. We found that temperature had a small positive median effect

365   (2.88 cases/°C, Wilcox $P < 0.001$) on dengue incidence (Figure 5a). A positive effect

366   is expected for the temperature range in Puerto Rico (Mordecai *et al.* 2017) (Figure

367   6e, black dashed lines), although the effect was occasionally much stronger, both

368   positive and negative (Figure 5a, b). The large negative effects occurred only at the

369   highest temperature values (as predicted by mechanistic models of temperature-

370   dependent transmission), reinforced by a lower quantile regression with a strongly

371   negative slope (Figure 5b, bottom dashed red line). However, positive effects

372   occurred across the whole temperature range, which is limited to temperatures

373   below the 29°C optimal temperature for transmission estimated from mathematical

374   models and laboratory data (Mordecai *et al.* 2017).

375   Rainfall had a small negative median effect (−0.12 cases/mm, Wilcox $P <$

376   0.001), but occasionally had very large negative effects (Figure 5a, c). These large,

377   negative effects of rainfall on dengue occurred when there was less than 100 mm of

378   rain per week (Figure 5c), consistent with expectations that drought could lead to a

379   high number of dengue cases due to water storage, which can provide mosquito

380   breeding habitat (Oliveira-lima *et al.* 2000). There are also small positive effects of

381   rainfall on dengue (Figure 5c), suggesting that overall the results showed competing

382   effects of low to moderate rain providing standing water for mosquito breeding and

383   humans storing water where mosquitoes can breed when there is drought or low

384   rainfall.

385   These results suggest the strength and direction of the effects of climate on

386   dengue dynamics depend on the state of the system. In addition to the nonlinear

387   effects of climate drivers themselves on dengue incidence, another potential cause

388   of state-dependent climate effects on dengue dynamics is the variation in the

389   susceptible population size over time (Figure 6a, b). Outbreaks do not occur when

390   there are too few susceptible people in the population. As expected, when the

391   susceptibles index was small ($\lambda < 0.85$) incidence was insensitive to climate (Figure

392   6c, f). By contrast, when the susceptibles index was large ($\lambda > 0.85$), temperature

393   and rainfall effects on dengue incidence appeared (Figure 6d, g). The gradual

394   increase and decrease of the rate of change of dengue as a function of temperature

395   (Figure 6d, red solid lines) aligned well with the changes in slope over the

396   increasing part (Figure 6e, black dashed lines representing the temperature range in

397   our study) of the unimodal temperature response curve for dengue transmission by

398   *Ae. aegypti* developed previously (Mordecai *et al.* 2017). This is an important

399   finding, since evidence of climate functional responses for disease dynamics is rare

400   due to the difficulty of obtaining appropriately informative field data. It is possible

401   that if we had temperature data ranging across a larger spectrum—possibly by

402   assembling data across multiple climates—that the empirical functional response

403   derived from EDM would also look unimodal. Further, when the susceptibles index

404   was high, the slope of the relationship between rainfall and dengue incidence

405   became more negative as rainfall increased, suggesting a concave-down effect of

406   rainfall on incidence (Figure 6g, h). This relationship has been difficult to

407   characterize in the field because of multiple, possibly context-dependent and lagged,

408   mechanisms linking rainfall to dengue.

409   **DISCUSSION**

410   High host susceptibility allows seasonal climate suitability to fuel large dengue

411   epidemics in San Juan, Puerto Rico. The effects of climate and susceptibility are

412   nonlinear, interdependent, and state-dependent, which makes inference from

413   controlled experiments, equation-based mechanistic models, or phenomenological

414   models difficult. EDM provides methods for identifying these drivers, quantifying

415   their predictive power, and approximating their functional responses. In Puerto

416   Rico, the causes of extensive interannual variability in dengue incidence have

417   remained a mystery, despite hypotheses that climate and host susceptibility were

418   involved. Here, we used EDM and a proxy for susceptible availability to disentangle

419   nonlinear and interactive mechanisms driving disease dynamics.

420   We found that rainfall, susceptible availability, and plausibly temperature

421   (via its seasonality) interact to drive dengue incidence. Combined, these three

422   drivers predicted dengue incidence with high accuracy (Figure 4c). The EDM-based

423   forecasting model outperformed 16 models and an ensemble model in a recently

424   published dengue forecasting challenge (Johansson *et al.* 2019), suggesting that it

425   could enhance dengue control efforts if surveillance efforts continue to report

426   weekly case data. Finally, as expected from epidemiological theory, climate effects

427   on dengue only appeared when susceptible availability exceeded a threshold ($\lambda >$

428   0.85; Figure 6).

429   The fact that climate effects are first observed when $\lambda \approx 0.85$ (before the

430   onset of an outbreak, $\lambda = 1$), suggests that rainfall, and possibly temperature, have

431   an effect on the timing of an impending epidemic. Climate could drive the

432   transmission rate, thus influencing λ (which is proportional to both susceptible

433   population size and R_0 when λ is close to 1), and therefore the timing of an outbreak

434   could be attributed to the changes in transmission caused by seasonal climatic

435   drivers (Rypdal & Sugihara 2019). The seasonality of temperature and rainfall had

436   higher predictive skill than seasonality of susceptibles index (Figures 3 and S8, grey

437   lines), further supporting that seasonality of incidence was associated with climate.

438   However, the susceptibles index was critical for predicting dengue epidemic

439   magnitudes (Figure 4c–f). Using the same data, Johnson *et al.* (2018) found that

440   mechanistic models could predict the timing of seasonal epidemics, but that a

441   phenomenological machine learning component was needed to capture interannual

442   variation in epidemic magnitude. Our work suggests that the unobserved size of the

443   susceptible population was a key missing link for predicting magnitude variation

444   across years.

445   Previous studies have built models accounting for both susceptible

446   availability and climate on dengue by reconstructing time series of susceptibles

447   from a compartmental modeling framework (Metcalf *et al.* 2017). However, no

448   previous studies on dengue have explored the interdependence between climate

449   and susceptible population size. We showed that susceptible availability modifies

450   climate effects on dengue: climate has negligible effects unless the susceptible

451   population size is large enough (Figure 6). The interdependence of climate and

452   population susceptibility has also been studied in diseases where the opposite effect

453   was found. For example, climate effects on SARS-CoV-2 are expected to be negligible

454   when susceptible availability is high in the early stage of the emerging pandemic

455   (Baker *et al.* 2020). For influenza dynamics, population density in cities—potentially

456   a proxy for susceptible availability—also modulated climate effects on disease

457   transmission: climate effects were negligible in cities with high population densities

458   (Dalziel *et al.* 2018).

459   Because dengue susceptibility is so complex—due to the serotype dynamics

460   and time- and antibody titer-dependent cross-protection and enhancement

461   (Katzelnick *et al.* 2017b)—total population density or size may not be a reasonable

22

462   proxy for susceptible availability in dengue dynamics, and a direct mechanistic

463   estimate of population susceptibility will likely never be widely available for most

464   populations. Accordingly, it has been difficult for previous mechanistic models to

465   capture susceptible dynamics for dengue and their interactions with climate.

466   However, our approach provides a useful proxy that captures the susceptible

467   population dynamics even in the absence of more detailed immunological

468   information. By inferring the susceptibles index from incidence data, we were able

469   to capture the strong influence of the susceptible availability on dengue dynamics,

470   which in turn moderated the effect of climate on dengue dynamics. This result is

471   expected from theory (Kermack & McKendrick 1927; Xu *et al.* 2017), but

472   demonstrating it empirically is a unique contribution of this study.

473   Even when accounting for susceptible availability, the effects of temperature

474   and rainfall on dengue were strongly state-dependent (Figure 6d, g). This result is

475   potentially due to nonlinear effects of each climate driver (Figure 6e, h), interactions

476   and correlations between temperature and rainfall, microclimate variation over

477   space and time that is not captured by weekly averages, and complex lagged effects

478   that are not captured by a single fixed lag (e.g., 9 weeks). In Puerto Rico, mosquitoes

479   also breed in septic tanks year-round, allowing transmission to occur independently

480   from rainfall (Mackay *et al.* 2009), thus weakening the rainfall–dengue negative

481   relationship (Figure 6g). Some of this additional variation may be captured in the

482   dengue incidence time series itself, which may explain why including it improves

483   forecast skill over climate and susceptibility alone (Figure 4e, f). Despite this

484   additional variation, our results are consistent with previous studies suggesting that

23

485   dengue dynamics in Puerto Rico are positively associated with temperature

486   (Johansson *et al.* 2009b; Barrera *et al.* 2011; Morin *et al.* 2015), and possibly

487   negatively associated with rainfall (Johansson *et al.* 2009a; Morin *et al.* 2015), since

488   most *Ae. aegypti* pupae in Puerto Rico are produced in human-made containers

489   during periods of drought (Barrera *et al.* 2011).

490   The climate and incidence data used here have been used in multiple

491   forecasting efforts, where ensemble approaches and approaches that incorporated

492   mechanisms outperformed purely statistical approaches (Johansson *et al.* 2019).

493   However, even the high-performing forecasting methods using the same dataset,

494   and including (experimentally-derived) assumed mechanisms for the joint influence

495   of climate and susceptibility on dengue dynamics, are still error-prone to the timing

496   (on the order of weeks) and the magnitude (on the order of 50 cases) of intra-

497   annual epidemics (Morin *et al.* 2015; Johansson *et al.* 2019). Mechanisms isolated

498   independently in controlled experiments do not necessarily scale up to the

499   population level, and susceptible dynamics derived from compartmental models

500   may be too simple to properly capture true susceptibility at the population level for

501   dengue (Katzelnick *et al.* 2017b). EDM allowed us to infer mechanisms empirically

502   from population-level data, and accounted for the population-level interdependence

503   between climate and susceptible availability for forecasting, which probably

504   contributed to our model outperforming previous forecasting models and

505   ensembles (Table S1).

506   Connecting climate and dengue at the population level is challenging,

507   because relationships are likely nonlinear and state-dependent. Rigorous methods

508   for testing hypotheses, deriving mechanisms, and making predictions is essential for

509   understanding disease dynamics. Our approach, using EDM and an inferred proxy

510   for the susceptible population size, confirmed that climate has nonlinear, seasonal

511   effects on dengue epidemics in San Juan, Puerto Rico, but only above a certain

512   threshold of susceptible availability. EDM-derived mechanisms could be applied to

513   predict ecological responses to changing environments in a world undergoing rapid

514   environmental change.

ACKNOWLEDGEMENTS

REFERENCES

Anderson, R.M. & May, R.M. (1979). Population biology of infectious diseases: Part I. *Nature,* 280, 361–367.

Baker, R.E., Yang, W., Vecchi, G.A., Metcalf, C.J.E. & Grenfell, B.T. (2020). Susceptible supply limits the role of climate in the early SARS-CoV-2 pandemic. *Science*, 369, 315–319.

Barrera, R., Amador, M. & MacKay, A.J. (2011). Population dynamics of *Aedes aegypti* and dengue as influenced by weather and human behavior in san juan, puerto rico. *PLoS Negl. Trop. Dis.*, 5, e1378.

Baskerville, E.B. & Cobey, S. (2017). Does influenza drive absolute humidity? *Proc. Natl. Acad. Sci.*, 114, 201700369.

Brady, O.J., Gething, P.W., Bhatt, S., Messina, J.P., Brownstein, J.S., Hoen, A.G., *et al.* (2012). Refining the Global Spatial Limits of Dengue Virus Transmission by Evidence-Based Consensus. *PLoS Negl. Trop. Dis.*, 6, e1760.

Caldwell, J., LaBeaud, D., Lambin, E., Stewart-Ibarra, A., Ndenga, B., Mutuku, F., *et al.* (2020). Climate explains geographic and temporal variation in mosquito-borne disease dynamics on two continents. *bioRxiv*, 2020.02.07.938720.

Cenci, S., Sugihara, G. & Saavedra, S. (2019). Regularized S-map for inference and forecasting with noisy ecological time series. *Methods Ecol. Evol.*, 2041–210X.13150.

Chen, S.C., Liao, C.M., Chio, C.P., Chou, H.H., You, S.H. & Cheng, Y.H. (2010). Lagged

552   temperature effect with mosquito transmission potential explains dengue

553   variability in southern Taiwan: Insights from a statistical analysis. *Sci. Total*

554   *Environ.*, 408, 4069–4075.

555   Cobey, S. & Baskerville, E.B. (2016). Limits to causal inference with state-space

556   reconstruction for infectious disease. *PLoS One*, 11, 1–22.

557   Cummins, B., Gedeon, T. & Spendlove, K. (2015). On the Efficacy of State Space

558   Reconstruction Methods in Determining Causality. *SIAM J. Appl. Dyn. Syst.*, 14,

559   335–381.

560   Dalziel, B.D., Kissler, S., Gog, J.R., Viboud, C., Bjørnstad, O.N., Metcalf, C.J.E., *et al.*

561   (2018). Urbanization and humidity shape the intensity of influenza epidemics

562   in U.S. cities. *Science*, 362, 75–79.

563   Deyle, E.R., Fogarty, M., Hsieh, C., Kaufman, L., Maccall, A.D. & Munch, S.B. (2013).

564   Predicting climate effects on Pacific sardine. *Proc. Natl. Acad. Sci. U. S. A.*, 110,

565   6430–6435.

566   Deyle, E.R., Maher, M.C., Hernandez, R.D., Basu, S. & Sugihara, G. (2016a). Global

567   environmental drivers of influenza. *Proc. Natl. Acad. Sci.*, 113, 13081–13086.

568   Deyle, E.R., May, R.M., Munch, S.B. & Sugihara, G. (2016b). Tracking and forecasting

569   ecosystem interactions in real time. *Proc. R. Soc. B Biol. Sci.*, 283.

570   Deyle, E.R. & Sugihara, G. (2011). Generalized theorems for nonlinear state space

571   reconstruction. *PLoS One*, 6.

572   Dixon, P.A., Milicich, M.J. & Sugihara, G. (1999). Episodic fluctuations in larval supply.

573   *Science*, 283, 1528–1530.

574   Dushoff, J., Plotkin, J.B., Levin, S.A. & Earn, D.J.D. (2004). Dynamical resonance can

575   account for seasonality of influenza epidemics. *Proc. Natl. Acad. Sci. U. S. A.*, 101,

576   16915–16916.

577   Ebisuzaki, W. (1997). A method to estimate the statistical significance of a

578   correlation when the data are serially correlated. *J. Clim.*, 10, 2147–2153.

579   Erlanger, T.E., Keiser, J. & Utzinger, J. (2008). Effect of dengue vector control

580   interventions on entomological parameters in developing countries: A

581   systematic review and meta-analysis. *Med. Vet. Entomol.*

582   Gordon, A., Kuan, G., Mercado, J.C., Gresh, L., Avilés, W., Balmaseda, A., *et al.* (2013).

583   The Nicaraguan Pediatric Dengue Cohort Study: Incidence of Inapparent and

584   Symptomatic Dengue Virus Infections, 2004-2010. *PLoS Negl. Trop. Dis.*, 7,

585   e2462.

586   Grziwotz, F., Strauß, J.F., Hsieh, C. & Telschow, A. (2018). Empirical Dynamic

587   Modelling Identifies different Responses of *Aedes Polynesiensis* Subpopulations

588   to Natural Environmental Variables. *Sci. Rep.*, 8, 16768.

589   Hamel, R., Surasombatpattana, P., Wichit, S., Dauvé, A., Donato, C., Pompon, J., *et al.*

590   (2019). Phylogenetic analysis revealed the co-circulation of four dengue virus

591   serotypes in Southern Thailand. *PLoS One*, 14, e0221179.

592   Hii, Y.L., Zhu, H., Ng, N., Ng, L.C. & Rocklöv, J. (2012). Forecast of Dengue Incidence

593   Using Temperature and Rainfall. *PLoS Negl. Trop. Dis.*, 6, e1908.

594   Huber, J.H., Childs, M.L., Caldwell, J.M. & Mordecai, E.A. (2018). Seasonal

595   temperature variation influences climate suitability for dengue, chikungunya,

596   and Zika transmission. *PLoS Negl. Trop. Dis.*, 12, e0006451.

597   Jiménez-Silva, C.L., Carreño, M.F., Ortiz-Baez, A.S., Rey, L.A., Villabona-Arenas, C.J. &

598   Ocazionez, R.E. (2018). Evolutionary history and spatio-temporal dynamics of

599   dengue virus serotypes in an endemic region of Colombia. *PLoS One*, 13,

600   e0203090.

601   Johansson, M.A., Apfeldorf, K.M., Dobson, S., Devita, J., Buczak, A.L., Baugher, B., *et al.*

602   (2019). An open challenge to advance probabilistic forecasting for dengue

603   epidemics. *Proc. Natl. Acad. Sci.*, 116, 24268–24274.

604   Johansson, M.A., Cummings, D.A.T. & Glass, G.E. (2009a). Multiyear climate

605   variability and dengue - El Niño southern oscillation, weather, and dengue

606   incidence in Puerto Rico, Mexico, and Thailand: A longitudinal data analysis.

607   *PLoS Med.*, 6, e1000168.

608   Johansson, M.A., Dominici, F. & Glass, G.E. (2009b). Local and global effects of climate

609   on dengue transmission in Puerto Rico. *PLoS Negl. Trop. Dis.*, 3, e382.

610   Johansson, M.A., Reich, N.G., Hota, A., Brownstein, J.S. & Santillana, M. (2016).

611   Evaluating the performance of infectious disease forecasts: A comparison of

612   climate-driven and seasonal dengue forecasts for Mexico. *Sci. Rep.*, 6, 33707.

613   Johnson, L.R., Gramacy, R.B., Cohen, J., Mordecai, E., Murdock, C., Rohr, J., *et al.*

614   (2018). Phenomenological forecasting of disease incidence using

615   heteroskedastic gaussian processes: A dengue case study. *Ann. Appl. Stat.*, 12,

616   27–66.

617   Katzelnick, L.C., Coloma, J. & Harris, E. (2017a). Dengue: knowledge gaps, unmet

618   needs, and research priorities. *Lancet Infect. Dis.*, 17, e88–e100.

619   Katzelnick, L.C., Gresh, L., Halloran, M.E., Mercado, J.C., Kuan, G., Gordon, A., *et al.*

620   (2017b). Antibody-dependent enhancement of severe dengue disease in

621   humans. *Science*, 358, 929–932.

622   Kermack, W.O. & McKendrick, A.G. (1927). A Contribution to the Mathematical

623   Theory of Epidemics. *Proc. R. Soc. A Math. Phys. Eng. Sci.*, 115, 700–721.

624   Kilpatrick, A.M. & Randolph, S.E. (2012). Drivers, dynamics, and control of emerging

625   vector-borne zoonotic diseases. *Lancet.*

626   Koenraadt, C.J.M. & Harrington, L.C. (2008). Flushing effect of rain on container-

627   inhabiting mosquitoes *Aedes aegypti* and *Culex pipiens* (Diptera: *Culicidae*). *J.*

628   *Med. Entomol.*, 45, 28–35.

629   Kraemer, M.U.G., Reiner, R.C., Brady, O.J., Messina, J.P., Gilbert, M., Pigott, D.M., *et al.*

630   (2019). Past and future spread of the arbovirus vectors *Aedes aegypti* and *Aedes*

631   *albopictus*. *Nat. Microbiol.*, 4, 854–863.

632   Kraemer, M.U.G., Sinka, M.E., Duda, K.A., Mylne, A.Q.N., Shearer, F.M., Barker, C.M., *et*

633   *al.* (2015). The global distribution of the arbovirus vectors *Aedes aegypti* and

634   *Ae. Albopictus*. *Elife*, 4.

635   Lambrechts, L., Paaijmans, K.P., Fansiri, T., Carrington, L.B., Kramer, L.D., Thomas,

636   M.B., *et al.* (2011). Impact of daily temperature fluctuations on dengue virus

637   transmission by *Aedes aegypti*. *Proc. Natl. Acad. Sci. U. S. A.*, 108, 1–6.

638   Liu-Helmersson, J., Stenlund, H., Wilder-Smith, A. & Rocklöv, J. (2014). Vectorial

639   capacity of *Aedes aegypti*: Effects of temperature and implications for global

640   dengue epidemic potential. *PLoS One*, 9.

641   Mackay, A.J., Amador, M., Diaz, A., Smith, J. & Barrera, R. (2009). Dynamics of *Aedes*

642   *aegypti* and *Culex quinquefasciatus* in Septic Tanks. *J. Am. Mosq. Control Assoc.*,

643   25, 409–416.

644   McLeod, A.I. (2011). Kendall: Kendall rank correlation and Mann-Kendall trend test.

645   Metcalf, C.J.E., Walter, K.S., Wesolowski, A., Buckee, C.O., Shevliakova, E., Tatem, A.J.,

646   *et al.* (2017). Identifying climate drivers of infectious disease dynamics: Recent

647   advances and challenges ahead. *Proc. R. Soc. B Biol. Sci.*

648   Mina, M.J., Metcalf, C.J.E., De Swart, R.L., Osterhaus, A.D.M.E. & Grenfell, B.T. (2015).

649   Long-term measles-induced immunomodulation increases overall childhood

650   infectious disease mortality. *Science*, 348, 694–699.

651   Mordecai, E.A., Caldwell, J.M., Grossman, M.K., Lippi, C.A., Johnson, L.R., Neira, M., *et*

652   *al.* (2019). Thermal biology of mosquito-borne disease. *Ecol. Lett.*, ele.13335.

653   Mordecai, E.A., Cohen, J.M., Evans, M. V., Gudapati, P., Johnson, L.R., Lippi, C.A., *et al.*

654   (2017). Detecting the impact of temperature on transmission of Zika, dengue,

655   and chikungunya using mechanistic models. *PLoS Negl. Trop. Dis.*, 11,

656   e0005568.

657   Morin, C.W., Monaghan, A.J., Hayden, M.H., Barrera, R. & Ernst, K. (2015).

658   Meteorologically driven simulations of dengue epidemics in San Juan, PR. *PLoS*

659   *Negl. Trop. Dis.*, 9, e0004002.

660   Munch, S.B., Brias, A., Sugihara, G. & Rogers, T.L. (2020). Frequently asked questions

661   about nonlinear dynamics and empirical dynamic modelling. *ICES J. Mar. Sci.*,

662   77, 1463–1479.

663   Oliveira-lima, W., Hodgson, J.C., Pontes, R.J.S. & Freeman, J. (2000). Vector densities

664   that potentiate dengue outbreaks in a Brazilian city. *Trop. Med.*, 62, 378–383.

665   Park, J., Smith, C., Sugihara, G. & Deyle, E.R. (2020). rEDM: Empirical Dynamic

666   Modeling ('EDM'). R package version 1.6.1.

667   Pitzer, V.E., Viboud, C., Alonso, W.J., Wilcox, T., Metcalf, C.J., Steiner, C.A., *et al.* (2015).

668   Environmental Drivers of the Spatiotemporal Dynamics of Respiratory

669   Syncytial Virus in the United States. *PLoS Pathog.*, 11, 1–14.

670   Robert, M.A., Christofferson, R.C., Weber, P.D. & Wearing, H.J. (2019). Temperature

671   impacts on dengue emergence in the United States: Investigating the role of

672   seasonality and climate change. *Epidemics*, 28.

673   Ryan, S.J., Carlson, C.J., Mordecai, E.A. & Johnson, L.R. (2019). Global expansion and

674   redistribution of *Aedes*-borne virus transmission risk with climate change. *PLoS*

675   *Negl. Trop. Dis.*, 13, e0007213.

676   Rypdal, M. & Sugihara, G. (2019). Inter-outbreak stability reflects the size of the

677   susceptible pool and forecasts magnitudes of seasonal epidemics. *Nat.*

678   *Commun.*, 10, 2374.

679   dos Santos, T.P., Cruz, O.G., da Silva, K.A.B., de Castro, M.G., de Brito, A.F., Maspero,

680   R.C., *et al.* (2017). Dengue serotype circulation in natural populations of *Aedes*

681   *aegypti*. *Acta Trop.*, 176, 140–143.

682   Sridhar, S., Luedtke, A., Langevin, E., Zhu, M., Bonaparte, M., Machabert, T., *et al.*

683   (2018). Effect of Dengue Serostatus on Dengue Vaccine Safety and Efficacy. *N.*

684   *Engl. J. Med.*, 379, 327–340.

685   Stewart Ibarra, A.M., Ryan, S.J., Beltrá N, E., Mejía, R.L., Silva, M. & Muñ Oz, N. (2013).

686   Dengue Vector Dynamics (*Aedes aegypti*) Influenced by Climate and Social

687   Factors in Ecuador: Implications for Targeted Control. *PLoS One*, 8.

688   Sugihara, G. (1994). Nonlinear forecasting for the classification of natural time

689   series. *Philos. Trans. R. Soc. A Math. Phys. Eng. Sci.*, 348, 477–495.

690   Sugihara, G., Deyle, E.R. & Ye, H. (2017). Reply to Baskerville and Cobey:

691   Misconceptions about causation with synchrony and seasonal drivers. *Proc.*

692   *Natl. Acad. Sci.*, 114, 201700998.

693   Sugihara, G., May, R., Ye, H., Hsieh, C., Deyle, E., Fogarty, M., *et al.* (2012). Detecting

694   Causality in Complex Ecosystems. *Science*, 338, 496–500.

695   Sugihara, G. & May, R.M. (1990). Nonlinear forecasting as a way of distinguishing

696   chaos from measurement error in time series. *Nature,* 344, 734–741.

697   Takens, F. (1981). Detecting strange attractors in turbulence. In: *Dynamical Systems*

698   *and Turbulence, Warwick 1980, Lecture Notes in Mathematics* (eds. Rand, D. &

699   Young, L.-S.). Springer, Berlin, Heidelberg., pp. 366–381.

700   Tran, A., L'Ambert, G., Lacour, G., Benoît, R., Demarchi, M., Cros, M., *et al.* (2013). A

701   rainfall- and temperature-driven abundance model for *Aedes albopictus*

702   populations. *Int. J. Environ. Res. Public Health*, 10, 1698–1719.

703   Trapletti, A. & Hornik, K. (2018). tseries: Time Series Analysis and Computational

704   Finance.

705   Watts, D.M., Burke, D.S., Harrison, B.A., Whitmire, R.E. & Nisalak, A. (1987). Effect of

706   temperature on the vector efficiency of *Aedes aegypti* for dengue 2 virus. *Am. J.*

707   *Trop. Med. Hyg.*, 36, 143–152.

708   Xu, L., Stige, L.C., Chan, K.-S., Zhou, J., Yang, J., Sang, S., *et al.* (2017). Climate variation

709   drives dengue dynamics. *Proc. Natl. Acad. Sci.*, 114, 113–118.

710   Zhao, S., Musa, S.S., Hebert, J.T., Cao, P., Ran, J., Meng, J., *et al.* (2020). Modelling the

711   effective reproduction number of vector-borne diseases: The yellow fever

712   outbreak in Luanda, Angola 2015-2016 as an example. *PeerJ*, 2020.

713
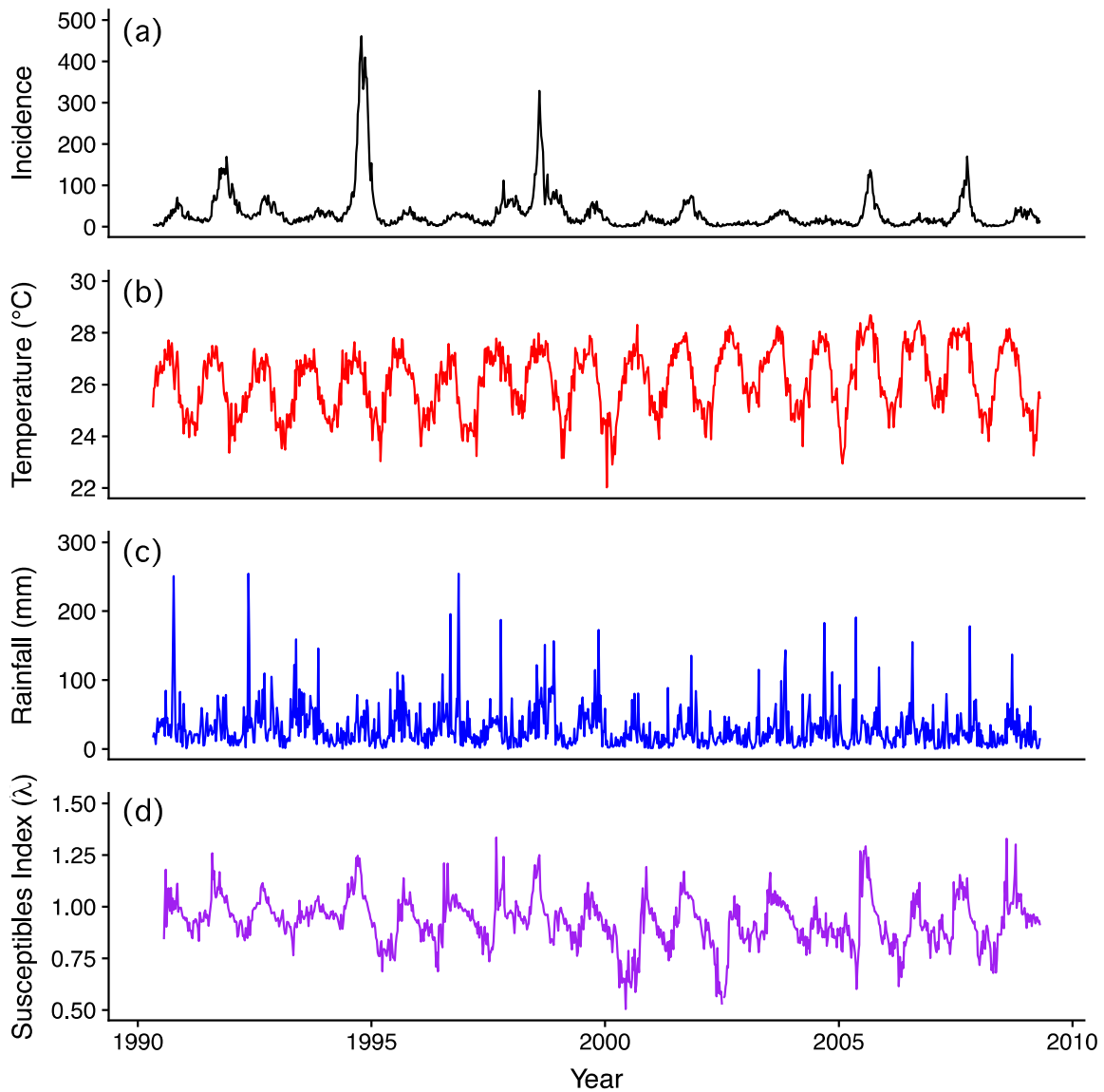
FIGURES

Figure 1. Dengue incidence, climate, and susceptibles index data. Time series (seasons 1990/1991–2008/2009) of (a) weekly dengue incidence (i.e., total number of cases per week), (b) weekly average temperature, (c) total weekly rainfall, and (d) a proxy for susceptible population size (see Supporting Information for details) in San Juan, Puerto Rico.

36

721
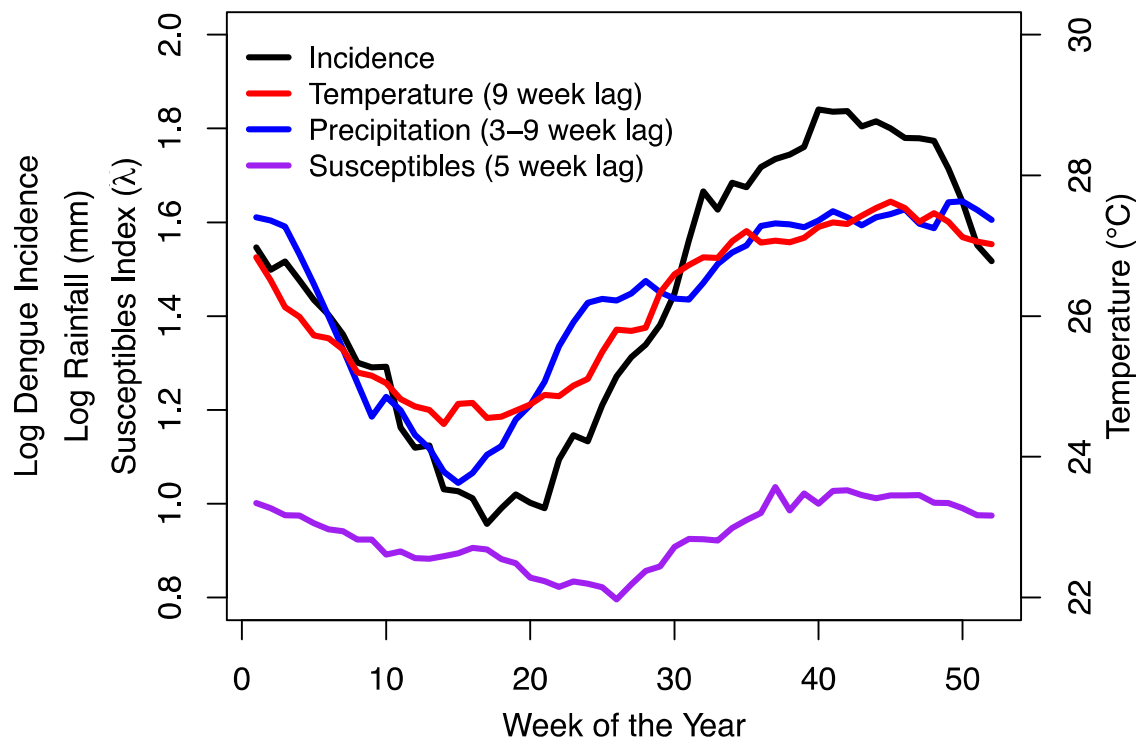
Figure 2. **Seasonal trends and lags of dengue incidence and its drivers.** The strong seasonal signal of dengue cases and other variables suggests potential causal lags between dengue incidence and temperature, rainfall, or the proxy for the susceptible population size. The lines represent interannual averages for each week of the year (i.e., calendar week) of dengue incidence (black), temperature shifted 9 weeks forward in time (red), average rainfall over the preceding 3–9 weeks and shifted 3 weeks forward in time (blue), and susceptibles index shifted 5 weeks forward in time (purple).

730
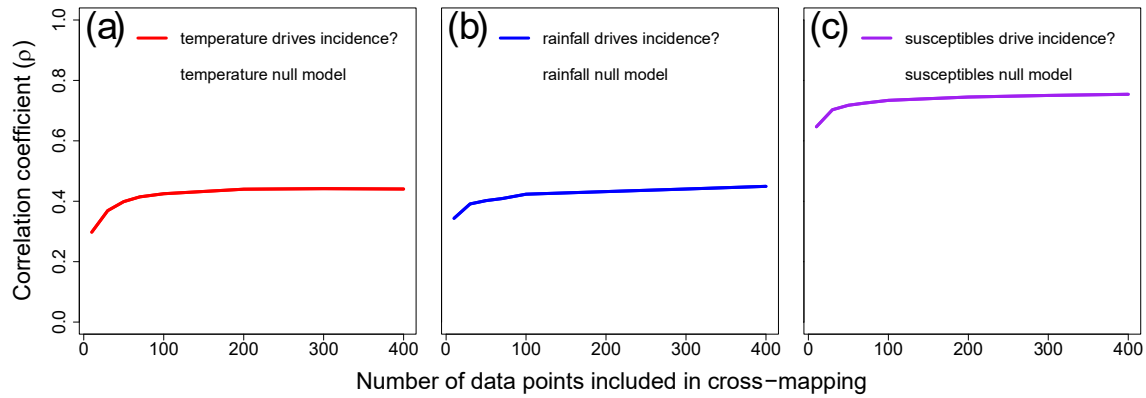
Figure 3. Climate and susceptibles index drive dengue incidence. Cross-mapping between dengue incidence and temperature (a; red), rainfall (b; blue), or susceptibles index (c; purple) display significant (Kendall's $\tau > 0$; $P < 0.01$) convergence in cross-mapping skill (i.e., ρ increases and reaches an asymptote) as the length of the time series increases (a signal of putative causality). Red, blue and purple shaded regions represent the 0.025 and 0.975 quantiles of bootstrapped time series segments. Grey shaded regions represent the 0.025 and 0.975 quantiles of the seasonal null distributions obtained from 500 runs of randomized time series with conserved seasonal trends (Deyle *et al.* 2016a). Solid lines represent medians of distributions. Rainfall and susceptibles index showed significant forcing above and beyond seasonal signal (K-S $P < 0.0001$), because cross-mapping of the true time series (blue and purple) are distinguishable from their respective null models (grey), whereas temperature forcing was not distinguishable from the null (K-S $P = 0.90$).
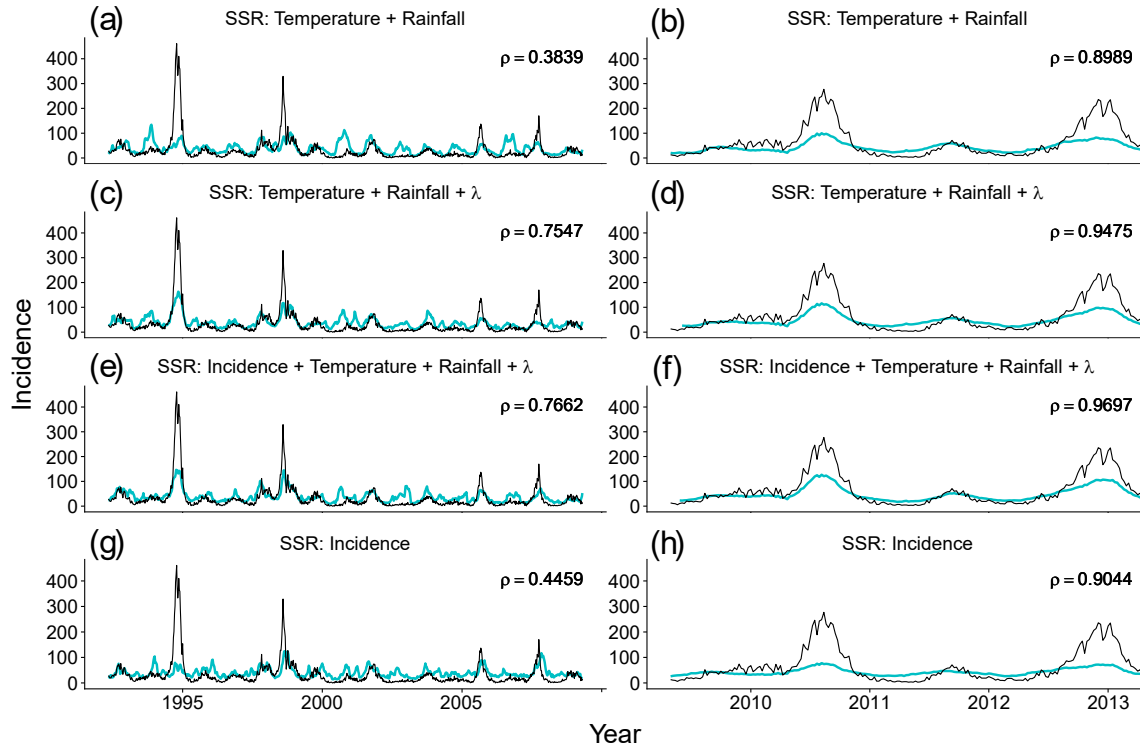
745

Figure 4. Predictive power of climate and susceptibles index (λ) on in-sample (left) and out-of-sample (right) dengue incidence. Forecasting results of incidence (8 weeks ahead) are shown in turquoise (solid lines represent the mean; shaded regions represent 90% confidence intervals) and observed incidence in black. (a, c, e, g) Time series for seasons 1990/1991–2008/2009 were used to construct SSR models for forecasts using leave-one-out cross-validation. (b, d, f, h) Data for seasons 2009/2010–2012/2013 were used to evaluate the SSR models constructed in a, c, e, and g, respectively, for out-of-sample forecasts. All SSR models (a–h) had significant forecasting skill (ρ) values (Fisher's z-transformation $P <$ 0.001).
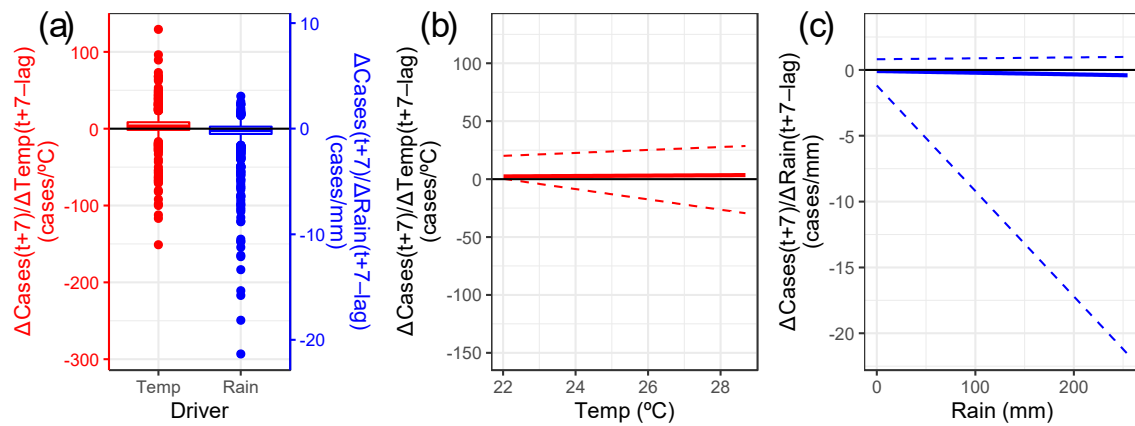
Figure 5. Temperature and rainfall show mixed effects on dengue incidence.
Scenario exploration quantified the variable effect of changes in drivers on dengue. Boxplots show that the median effects of rainfall (Rain) and temperature (Temp) are small (close to zero), but drivers occasionally have strong impacts (a). To investigate climate driver functional responses, we plotted the rate of change of dengue incidence as a function of temperature (b) and rainfall (c). Red and blue lines represent regression on the median for temperature and rainfall, respectively, in a quantile regression. The dashed red and blue lines represent regression on the 0.05 and 0.95 quantiles of temperature and rainfall, respectively. Temperature has an overall positive effect on dengue incidence (median regression line of the rate of change is positive), but can also have large negative and positive effects (a, b). Rainfall has an overall negative effect (median regression line of the rate of change is negative), but can also have small positive and large negative effects (a, c).
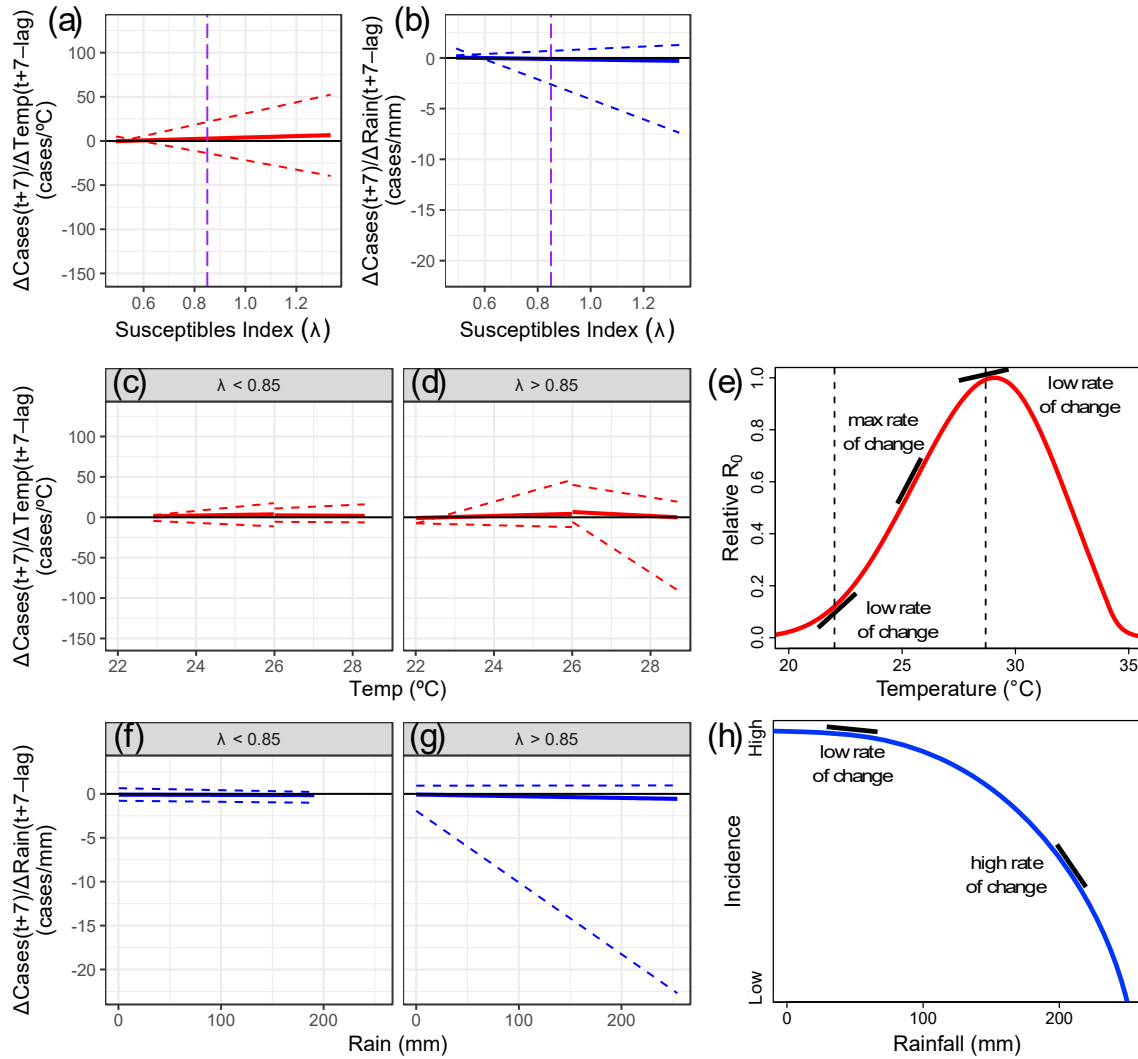
40

Figure 6. Temperature and rainfall effects on dengue incidence vary depending on the susceptible population size (λ). The effect of changes in temperature (a) and rainfall (b) against λ shows that driver effects are split around the threshold $\lambda \approx 0.85$ (purple dashed line). The red and blue lines represent the median regression of temperature and rainfall effects, respectively, in a quantile regression (a–d, f, g). The dashed red and blue lines represent the 0.05 and 0.95 quantile regressions of temperature and rainfall effects, respectively (a–d, f, g). Neither driver has an effect on dengue incidence when susceptible availability is low

41

779   ($\lambda < 0.85$; c, f). However, when $\lambda > 0.85$ climate effects are observed: temperature

780   has mostly a positive effect (d), possibly sigmoidal in that temperature range (e),

781   and rainfall has a negative effect (g), and conceptually a concave down functional

782   response (h; black lines represent tangents, where the slope of the tangent is the

783   rate of change). The effect of temperature on relative R_0 of dengue assuming

784   transmission via *Aedes aegypti* mosquitoes is unimodal (Mordecai *et al.* 2017) over a

785   large temperature range (e; dashed lines indicate the minimum and maximum

786   temperature values in the data of our study, black lines represent tangents, where

787   the slope of the tangent is the rate of change of relative R_0 of dengue as a function of

788   temperature). Assuming that relative R_0 is proportional to dengue incidence, our

789   results suggest that the rate of change of dengue incidence is increasing until

790   reaching a maximum and then decreasing (d; red median regression lines).

791   However, even when driver effects are split at the evident threshold of $\lambda = 0.85$ (c,

792   d, f, g), there are still many occurrences when the susceptible population size is

793   sufficient large ($\lambda > 0.85$) but temperature and rainfall have no effect. In certain

794   cases, temperature has even a negative effect on dengue (d).